SCIENTIFIC REPORTS

OPEN

SUBJECT AREAS:
PROTEIN AGGREGATION
MASS SPECTROMETRY

Received
19 August 2013

Accepted
4 November 2013

Published
20 November 2013

Correspondence and requests for materials should be addressed to J.A.A. (aquilina@uow.edu.au)

Glutathionylation potentiates benign superoxide dismutase 1 variants to the toxic forms associated with amyotrophic lateral sclerosis

Luke McAlary[1,2], Justin J. Yerbury[1,2] & J. Andrew Aquilina[1,2]

[1]Illawarra Health and Medical Research Institute, [2]School of Biological Sciences, University of Wollongong, Northfields Avenue, Wollongong NSW, Australia 2522.

Dissociation of superoxide dismutase 1 dimers is enhanced by glutathionylation, although the dissociation constants reported to date are imprecise. We have quantified the discreet dissociation constants for wild-type superoxide dismutase 1 and six naturally occurring sequence variants, in their unmodified and glutathionylated forms, at the ratios expressed. Unmodified superoxide dismutase 1 variants that shared similar dissociation constants with $SOD1^{WT}$ had disproportionately increased dissociation constants when glutathionylated. This defines a key role for glutathionylation in superoxide dismutase 1 associated familial amyotrophic lateral sclerosis.

Approximately one in five cases of familial amyotrophic lateral sclerosis (fALS) is due to naturally occurring mutations in the gene encoding superoxide dismutase 1 (SOD1)[1]. Over 150 such mutations have been reported to occur, and these mutations can occur at virtually any residue of the primary sequence. Many of these mutations confer a significant level of instability upon the native dimer, which may ultimately unfold and form insoluble cytoplasmic aggregates - a hallmark of SOD1 associated fALS pathology[2]. Recently, evidence has emerged to suggest that $SOD1^{WT}$ aggregation is also involved in some cases of the considerably more prevalent sporadic ALS[3–5].

The prevailing hypothesis of SOD1 aggregation suggests that dissociation of the native homodimer is a key step, as SOD1 monomers have been identified as a common misfolding intermediate[6,7]. This mechanism is supported by the extraordinary difference in dissociation constant (K_D) reported for the $SOD1^{A4V}$ dimer (3 μM)[8], compared with $SOD1^{WT}$ (2.25 nM)[9]; i.e. the dissociation of $SOD1^{A4V}$ into monomers is approximately 1000 times more facile at concentrations found *in vivo*. Furthermore, chemical cross-linking of the aggregation prone variant, $SOD1^{A4V}$ can prevent its aggregation *in vitro*[8], while cross-linking of other mutants conferred greater thermostability[10].

A compounding factor in SOD1 dissociation is the post-translational modification (PTM) of Cys111 by the ubiquitous antioxidant, glutathione (GSH), which has been demonstrated as being the dominant PTM in human tissue[9] (Fig. 1a; Fig. S1a). Similar to many residues in the primary chain of SOD1, Cys111[11] is proximal to the dimer interface and, not surprisingly, the introduction of GSH has been proposed to augment dissociation[11]. We explored this hypothesis for a set of human SOD1 variants with well-defined and broad ranging rates of disease progression; from 1.2 years survival post-onset for $SOD1^{A4V}$, to approximately 17.6 years for $SOD1^{H46R}$.

Results

Our initial assay, using mass spectrometry, revealed that all variants were glutathionylated to some extent when produced in *E. coli*, from a low of 3% for $SOD1^{V148G}$ to 36% for $SOD1^{A4V}$ (Fig. 1a). When these data were arranged in order of disease progression, a plausible correlation was evident for $SOD1^{A4V}$, $SOD1^{G93A}$, $SOD1^{G37R}$ and $SOD1^{H46R}$; however substantial glutathionylation of non-pathogenic $SOD1^{WT}$ compared to the aggressive variant $SOD1^{V148G}$, suggested that this modification alone is not predictive of disease progression. Indeed, while the sequence of these SOD1 variants may determine their susceptibility to glutathionylation, further work is required to confirm this in ALS patients.

To compare the relative dissociation propensity of our SOD1 variants, we performed nanoelectrospray-ionization mass spectrometry, with conditions optimized to preserve solution phase structures during ionization and subsequent *in vacuo* detection[12] (Fig. 1b; Fig. S2). Each of the SOD1 variant spectra exhibited peaks arising from two dominant ion populations at ~2900 *m/z* and ~3200 *m/z*, corresponding to the 10^+ and 11^+ ions of their respective dimers. Only minor peaks were observed for the 9^+ and 12^+ charge states, indicating that the dimers had negligible variation in their tertiary and quaternary structures. On closer inspection, a series of three maxima were identified within the 10^+ and 11^+ peaks, arising from dimers composed of; (i) two unmodified SOD1 (*u*SOD1) monomers; (ii) *u*SOD1 paired with *gs*SOD1; (iii) two *gs*SOD1 monomers. With the exception of $SOD1^{A4V}$, monomers were significantly less abundant than dimers, but similarly confined to two (7^+ and 8^+) charge states (Fig. 1b & inset). For all variants, the most abundant *monomer* observed was *gs*SOD1 (Fig. 1c), even though *u*SOD1 constituted the majority of total protein.

The mixture of SOD1 dimers was further interrogated using tandem mass spectrometry to isolate an ion population exclusive to the dimer (D^{11+}), prior to collision-induced dissociation (CID). At the minimum accelerating voltage (6 V) required to traverse an argon-filled CID region, the spectrum contained a single large peak of isolated D^{11+} ions (Fig. S3a). At an accelerating potential of 20 V, two additional peaks arose at ~2700 *m/z* and 3200 *m/z*, being due to the dissociation of D^{11+} into charge-complementary M^{5+} and M^{6+} monomers. These peaks increased in intensity at 40 V and 60 V, after which the more asymmetric dissociation pathway via M^{4+} and M^{7+} monomer ions became competitive. This hierarchical gas-phase molecular division, based on charge, was also observed for *gs*SOD1 (Fig. S3b). We compared the M^{6+} abundance for *u*SOD1 and *gs*SOD1 under low (10 V) versus high (70 V) energy CID conditions: at 10 V, $gsSOD1^{A4V}$, $gsSOD1^{G93A}$ and $gsSOD1^{G37R}$ had a greater proportion of M^{6+} than *u*SOD1 indicating that less energy is required to remove *gs*SOD1 monomer from the dimer than *u*SOD1. A comparison of the spectra at 70 V versus 10 V shows that *gs*SOD1:*u*SOD1 is larger at low energy CID for all seven proteins, which supports the hypothesis that modification by glutathione destabilizes the dimer.

A caveat to the gas-phase analysis of molecular interactions is the absence of bulk water which, to varying degrees, can affect the strength of non-covalent association between proteins[13]. Thus, it was possible that the more facile removal of *gs*SOD1 from the gas-phase dimer (Fig. 1b&c) is not necessarily reflective of the aqueous environment found *in vivo*. To address this uncertainty, we prepared dilution series of the SOD1 variants ranging from 20 μM down to 625 nM, prior to mass analysis using identical instrument conditions for all samples. The spectra acquired at each concentration provided a snapshot of all species present in solution and so, by plotting the proportion of monomer versus concentration (Fig. 2a; Fig. S4), we were able to calculate discreet dissociation constants for $(uSOD1)_2$ and $(gsSOD1)_2$ (Table 1; Fig. 2b). Unlike the homodimers, which dissociate into their respective and unique monomer pairs, products of the mixed dimer (*u*SOD1:*gs*SOD1) contributed to both populations of monomer, and were not so readily estimated. In an effort to account for monomers originating from the mixed dimer, we monitored the decline in (*u*SOD1:*gs*SOD1) $^{11+}$ ion intensity with successive dilution, and subtracted an equivalent quantity from each monomer signal. Although imprecise, we believe this correction attenuated, to some extent, the confounding effects of the mixed dimer species.

All *u*SOD1 variants had K_D values greater than $uSOD1^{WT}$ (9 ± 1 nM), implying that these single residue substitutions are sufficient to disturb the quaternary structure (Table 1). The most substantial augmentation was observed for $uSOD1^{A4V}$ (1.1 ± 0.1 μM), being approximately 100-fold greater than $uSOD1^{WT}$,

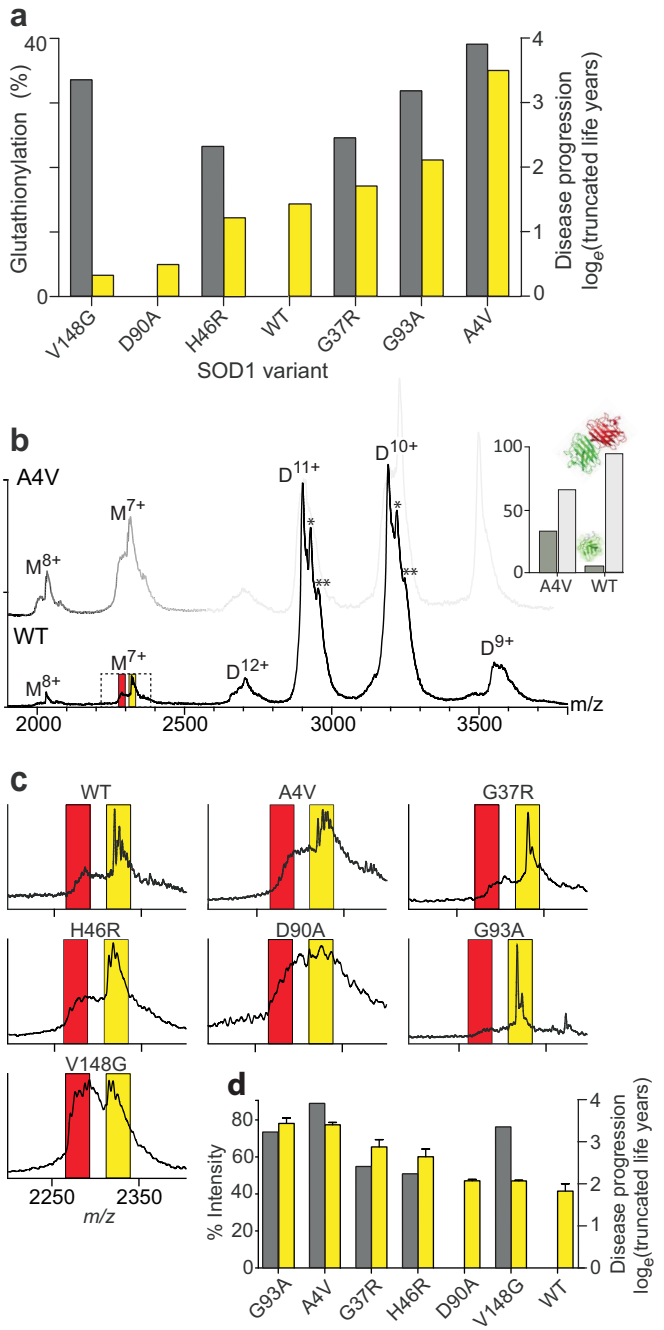

Figure 1 | Mass spectrometry analysis of SOD1 variants. (a) Percentage of recombinantly expressed SOD1 that was glutathionylated (yellow), as determined by the area under the peaks of MS spectra, compared to disease progression (grey), expressed in truncated life years as $\log_e[(75 - (25 + d)]$, where d equals the reported average disease duration, assumed life expectancy is 75 years and age at onset of disease is set to 50 years. (b) Mass spectrum of native $SOD1^{WT}$ (main) and $SOD1^{A4V}$ (faint) with species charge states labeled (D = dimer, M = monomer). Additional maxima within the peaks are the result of glutathionylation of one or both subunits to give a mixed (*) or *gs*SOD1(**) dimer. Inset shows the ratio of dimer to monomer for the two proteins, derived from charge state peak areas in the spectrum. (c) Expansion of the M^{7+} region showing peaks corresponding to *u*SOD1 (red) and *gs*SOD1 (yellow). (d) The percentage of *gs*SOD1 monomer (yellow) compared to disease progression (grey) for all SOD1 variants. The *gs*SOD1 measurements were performed in triplicate and error bars represent standard error of the mean.

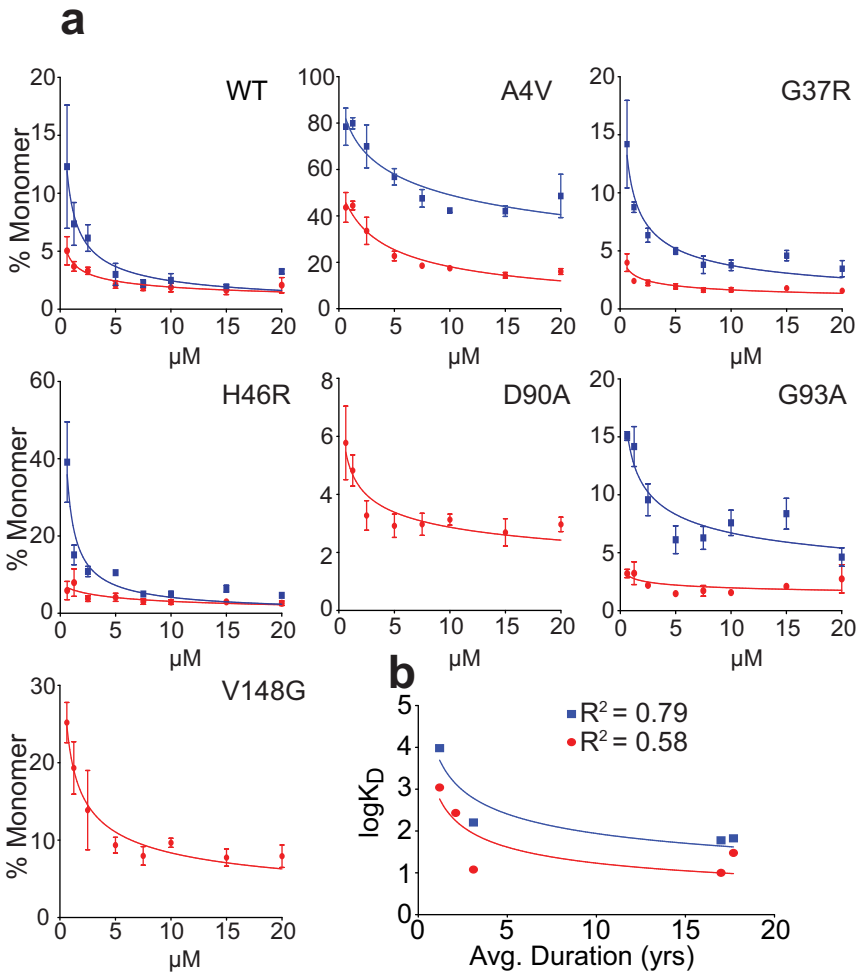

Figure 2 | SOD1 monomer abundance increases with dilution. (a) of SOD1 variants showing changes in the proportion of monomeric *u*SOD1 (red) and *gs*SOD1 (blue) as a function of protein concentration: (**i**) SOD^{WT}, (**ii**) SOD1^{A4V}, (**iii**) SOD1^{G37R}, (**iv**) SOD1^{H46R}, (**v**) SOD1^{D90A}, (**vi**) SOD1^{G93A}, (**vii**) SOD1^{V148G}. Analyses were performed in triplicate at each concentration and error bars represent standard deviation about the mean. (b) Relationship between disease duration and K_D for *u*SOD1 (red) and *gs*SOD1 (blue).

whereas *u*SOD1^{G93A} (12 ± 1 nM) had a K_D only marginally higher than *u*SOD1^{WT}. Significantly, the K_D value of each *gs*SOD1 species was higher than the corresponding *u*SOD1, with the largest (13-fold) increase observed for *gs*SOD1^{G93A}, followed by *gs*SOD1^{A4V} (9-fold), *gs*SOD1^{G37R} (6-fold) and *gs*SOD1^{WT} (4-fold) (Table 1). There was insufficient *gs*SOD1^{V148G} and *gs*SOD1^{D90A} to accurately calculate their K_D values.

Discussion

Glutathionylation of SOD1 expressed in *E. coli*, has previously been reported to occur at each of the four cysteine residues (Cys6, Cys57, Cys111, and Cys146) as detected by mass spectrometry[14]. Contrastingly, our analysis of recombinant SOD1^{WT} demonstrated that no more than one glutathione was bound per subunit, and this was the case for all SOD1 variants in this study (Fig. S1). This discrepancy stems from the protocol used by Furukawa and coworkers[14], which directed expression of SOD1 into inclusion bodies or soluble apo-proteins followed by refolding and metal enrichment after extraction from bacterial cells[15]. In the present work, SOD1 was co-expressed with the yeast-copper-chaperone for SOD1 (yCCS) in the presence of copper and zinc, with subsequent purification of soluble SOD1 from the bacterial cytosol[16]. The yCCS facilitates folding of the nascent chain, and formation of the disulfide bond between Cys57 and Cys146[14]. This disulfide effectively locks the β-barrel structure, rendering these Cys residues inaccessible to larger molecules; *ipso facto*, unlikely sites of glutathionylation. Furthermore, it has been demonstrated that Cys6 is buried inside the β-barrel of catalytically active SOD1, i.e., inaccessible to aqueous reductants[17]. We assessed the dismutase activity of our variants using in-gel zymography, which yielded positive results for all but the metal-binding site mutant,

Table 1 | SOD1 dissociation constants as determined by native mass spectrometry. The dissociation constants are means ± standard error from 3 distinct data sets with each containing 5 data points (see supplementary figure 4)

Variant	WT	A4V	G37R	H46R	D90A	G93A	V148G
SOD1 K_D (nM)	9 ± 1	1100 ± 100	10 ± 1	30 ± 4	25 ± 4	12 ± 1	271 ± 40
GS-SOD1 K_D (nM)	34 ± 5	9600 ± 900	60 ± 9	97 ± 16	-	160 ± 32	-

SOD1^{H46R} (Fig. S1b). Therefore, although we did not explicitly demonstrate Cys111 to be the site of our observed glutathionylation, it is inferable that the only cysteine residue sufficiently exposed and therefore substantially modified by glutathione was Cys111.

It is well documented that patients suffering from SOD1-associated fALS have variable survival times, dependent upon the particular amino acid mutation[18]. Considering the role played by dimer dissociation, as an entrée to aggregation, we scrutinized our data for evidence of a link between patient survival and K_D (Fig. 2b). For *u*SOD1, the K_D values were poorly associated with disease duration ($R^2 = 0.58$), primarily due to the outlier characteristics of *u*SOD1^{G93A}. In contrast, K_D values for *gs*SOD1 showed a much stronger correlation ($R^2 = 0.79$), indicating that glutathionylation may be responsible for the disparity between perceived SOD1 stability and observed patient survival. Consider the G93A mutation. This is reported as having little effect upon dimer dissociation[19], and our results for the K_D of *u*SOD1^{G93A} confirm this (Fig. 3a); yet the survival time of patients carrying this mutation is, on average, a mere 2.2 years. Our ability to distinguish between, and calculate separate K_D values for *u*SOD1 and *gs*SOD1 resolves this apparent inconsistency - the K_D of *gs*SOD1^{G93A} is *13 times higher* than that of *u*SOD1 (Fig. 3b; Table 1) - highlighting the significance of this methodology.

Our data can be used to reframe the original hypothesis in more specific terms: i.e., it is not only (the extent of) SOD1 glutathionylation that influences the rate of disease progression, but also the K_D of the glutathionylated species. Glutathionylation, however, is not a requirement for pathogenicity, as sequence modification alone of SOD1^{V148G} causes a 30-fold increase in K_D over SOD1^{WT}. Similarly, our extracted K_D value for *u*SOD1^{A4V} reflects the considerable instability of this non-glutathionylated species. These mutations are located deep in the inter-subunit cleft, where small molecular volume changes are able to disrupt the dimer interface leading to more facile dissociation[20] (Fig. S5).

In contrast to Val148 and Ala4, Gly37 and Gly93 are spatially remote to the dimer interface, being situated in the β3/β4 Greek key loop and β5/β6 inter-strand loop respectively (Fig. S5). It is notable that these loops are proximal to each other and the Leu38 cork, while Cys111 is within the β6/β7 Greek key loop at the opposite end of the β-barrel. Prior to glutathionylation, the individual mutations G37R and G93A impart negligible effect upon the K_D of SOD1; i.e., *in isolation, these mutations are not pathologically destabilizing* (Table 1). Rather, it is the synergy of glutathionylation and point mutation at the β-barrel 'poles' that accounts for the significantly higher K_D values reported in this study, and presumably, the malignance of these variants *in vivo*. It stands to reason then, that glutathionylation of SOD1 alters the K_D of a multitude of individual variants in a unique, allosteric-like fashion, and that it is the combination of $K_D^{(uSOD1)}$ and $K_D^{(gsSOD1)}$ (Fig. 3c) which impact the pathogenicity of the protein. Therefore, we propose an elaboration to the contemporary notion in which SOD1 dissociation is the primary underlying cause of SOD1 fALS.

Specifically, dissociation of the SOD1 dimer is a biophysical consequence of either, (i) a potent destabilizing mutation such as A4V, or (ii) glutathionylation of a weak or non-destabilizing mutation

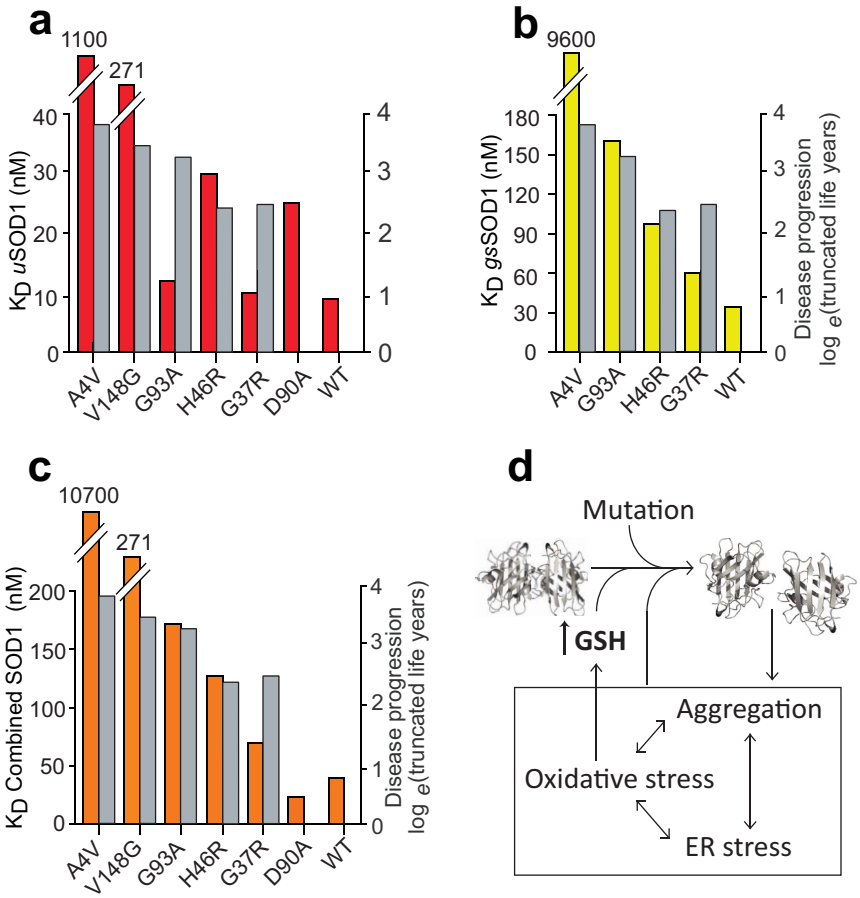

Figure 3 | The profound effect of glutathionylation on SOD1 dissociation constants. Histograms comparing K_D values of (a) *u*SOD1, (b) *gs*SOD1, and (c) *u*SOD1 + *gs*SOD1, to disease progression (grey). (d) A scheme of the proposed factors affecting SOD1 dimer dissociation. Briefly, dimer dissociation occurs due to mutation, glutathionylation, and cellular stresses. The increased monomer population is more likely to unfold and increase cellular stress. Glutathione (GSH) levels in the cell are elevated during periods of oxidative stress, thereby increasing the chances of SOD1 becoming glutathionylated.

such as G93A. Consequently, there is a twofold increase in the abundance of monomers, which are more susceptible to misfold into toxic conformations compared to the dimer[6,7] (Fig. 3d). If the cellular clearance rate of misfolded SOD1 is inadequate, increasingly frequent hydrophobic interactions ultimately give way to aggregation, forming larger amorphous structures that stress the cellular machinery[21]. Many neurodegenerative diseases, including ALS are also associated with oxidative stress[22], which in turn can lead to an up-regulation of glutathione[23]. Indeed, an increase in GSH has been observed in ALS patient CSF[24]. Analysis of human tissue from ALS patients, and in cell experiments, are currently under way to further investigate the role of glutathionylation in SOD1 associated fALS.

Methods

Materials. All solutions were prepared using Milli-Q ultra-purified water using the Millipore purification system (Massachusetts, USA). All materials were of analytical grade. Tryptone, Tris-base, DTT, β-mercaptoethanol, bromophenol blue, brilliant blue, ammonium persulphate, SDS, ampicillin sodium salt, and IPTG were from Amresco (Ohio, USA). NaCl, ammonium sulphate, agar, acetonitrile, Tris-HCl, tetramethylethylenediamine, ammonium acetate and RNase were from Sigma-Aldrich (Missouri, USA). DNase was from Roche Diagnostics (NSW, Australia). Carbenicillin was from Carbenicillin Direct (UK). Copper sulphate pentahydrate was from Ace Chemical Company (SA, Australia). Zinc sulphate heptahydrate was from Hopkin and Williams LTD (Birmingham, UK). Formic acid and acetic acid were from Univar (NSW, Australia). Methanol was from Ajax Finechem (NSW, Australia). Gold coated borosilicate electrospray capillaries were made in-house.

Expression and purification of recombinant SOD1. Plasmids encoding $SOD1^{WT}$, $SOD1^{A4V}$, $SOD1^{G37R}$, $SOD1^{H46R}$, $SOD1^{D90A}$, $SOD1^{G93A}$, and $SOD1^{V148G}$ were a gift from the Oliveberg Group (Sweden). Protein expression and purification were performed according to[16]. Briefly, the SOD1 plasmids were transformed into chemically competent BL21* *E. coli* using heat shock. Following transformation, the protein was expressed in the presence of copper and zinc ions with the addition of IPTG. The expressed SOD1 was purified via size exclusion chromatography (Hiload 16/60 Superdex 75 PG, GE USA) and anion exchange chromatography (Hiscreen Capto-Q, GE USA).

Sample preparation for mass spectrometry. SOD1 samples were desalted and buffer exchanged into 200 mM NH_4OAc (pH 7), using gel filtration chromatography (Superdex 200 10/300 GL, GE USA). Briefly, SOD1 samples were concentrated to 20 mg/ml and 100 µl was loaded onto the column at a flowrate of 0.4 mg/ml. The concentration of SOD1 was determined at 265 nm using a UV/Vis spectrophotometer, and a molar extinction coefficient of 18 700 $M^{-1}cm^{-1}$ [25].

Mass spectrometry. SOD1 samples in 200 mM NH_4OAc were denatured using formic acid and acetonitrile with the final concentration of each being 10% and 40% respectively. Mass analyses were performed on a Q-ToF ULTIMA mass spectrometer (Waters, UK) in positive ion mode with nanoelectrospray source. Instrument parameters included: capillary 1.5 kV, sample cone 200 V, desolvation gas flow 180 L/h. Native protein analyses were performed in 200 mM NH_4OAc on a SYNAPT G2 HDMS (Waters, UK) in positive ion mode. Instrument parameters were similar to Ruotolo et al. (2008)[26] with the exceptions: capillary voltage 1.5 kV, sample cone 30 V, cone gas 70 L/h, trap collision voltage 6 V, ion-transfer stage pressure 4.15 e^{-1} mbar, ToF analyzer pressure 2.38 e^{-6} mbar. All SOD1 variants were analyzed at a concentration of 20 µM. For MS/MS experiments, the trap collision energy was increased from 10 to 100 V in increments of 10 V with 30 scans at each increment. The dilution series mass spectra were acquired at concentrations of 20, 15, 10, 7.5, 5, 2.5, 1.25 and 0.625 µM with the following instrument parameters: capillary voltage 1.52 kV, sample cone 137 V, cone gas 78 L/h, trap collision voltage 16 V, transfer CE 8 V, ion transfer stage pressure 3.72 e^{-4} mbar, ToF analyser pressure 9.01 e^{-7} mbar, backing pressure 4.0 e^{0} mbar. All mass spectra in this study were externally calibrated using a solution of cesium iodide (10 mg/ml in water) and were processed using Masslynx 4.1 software (Waters, UK).

Dissociation constants. Dissociation constants were derived from the mass spectrometry data using the method of Rose et al., (2011)[27]. Briefly, the intensity, as determined by the area under the peak, of all peaks relating to SOD1 monomers (M_i) and dimers (D_i) were summed to give total signal intensity (I_{TS}):

$$I_M + I_D = I_{TS} \quad (1)$$

The proportion of monomer signal (P_M) was determined by dividing the intensity of the monomeric species (I_M) by the total signal intensity (I_{TS}):

$$I_M / I_{TS} = P_M \quad (2)$$

The concentration of monomer at equilibrium ($[M]_{eq}$) was determined by multiplying the proportion of monomer signal (P_M) by the total protein concentration in µM as determined by UV/Vis spectroscopy ($[P_o]$):

$$P_M \times [P_o] = [M]_{eq} \quad (3)$$

The concentration of dimer at equilibrium ($[D]_{eq}$) is defined as:

$$\left([P_o] - [M]_{eq}\right) \Big/ 2 = [D]_{eq} \quad (4)$$

The K_D was derived from the gradient of the plot of $[D]_{eq}$ against $[M]^2_{eq}$ (fitting performed with Prism 5.0, GraphPad Software, Inc.) In each case at least 5 data points were plotted with repeat experiments being performed if the line of best fit gave least-squares-regression, $R^2 < 0.75$.

Statistical analysis. Statistical analyses were carried out using Prism 5.0 software (Graphpad). All mass analyses were performed in triplicate (n = 3) with error bars representing the standard error of the mean. The dissociation plots (Figure 2) were fitted with a Log (Gaussian) function. The K_D plots (Fig. S4) were fitted using linear regression.

1. Valentine, J. S., Doucette, P. A. & Potter, S. Z. Copper-zinc superoxide dismutase and amyotrophic lateral sclerosis. *Annu. Rev. Biochem* **74**, 563–593 (2005).
2. Sibata, N., Asayama, K., Hirano, A. & Kobayashi, M. Immunohistochemical study on superoxide dismutases in spinal cords from autopsied patients with amyotrophic lateral sclerosis. *Dev. Neurosci.* **18**, 492–498 (1996).
3. Bosco, D. A. *et al.* Wild-Type and Mutant SOD1 Share an Aberrant Conformation and a Common Pathogenic Pathway in ALS. *Nat. Neurosci* **13**, 1396–1403 (2010).
4. Forsberg, K. *et al.* Novel antibodies reveal inclusions containing non-native SOD1 in sporadic ALS patients. *PLoS ONE* **5**, e11552 (2010).
5. Pokrishevsky, E. *et al.* Aberrant localization of FUS and TDP43 is associated with misfolding of SOD1 in Amyotrophic lateral sclerosis. *PLoS ONE* **7**, e35050 (2012).
6. Rakhit, R. *et al.* Monomeric Cu,Zn-superoxide Dismutase Is a Common Misfolding Intermediate in the Oxidation Models of Sporadic and Familial Amyotrophic Lateral Sclerosis. *J. Biol. Chem* **279**, 15499–15504 (2004).
7. Svensson, A. E. *et al.* Metal-free ALS variants of dimeric human Cu,Zn-superoxide dismutase have enhanced populations of monomeric species. *PLoS ONE* **5**, 1–10 (2010).
8. Ray, S. S. *et al.* An intersubunit disulfide bond prevents in vitro aggregation of a superoxide dismutase-1 mutant linked to familial Amyotrophic lateral sclerosis. *Biochem* **43**, 4899–4905 (2004).
9. Wilcox, K. C. *et al.* Modifications of Superoxide Disumutase (SOD1) in Human Erythrocytes: a Possible Role in Amyotrophic Lateral Sclerosis. *J. Biol. Chem* **284**, 13940–13947 (2009).
10. Auclair, J. R., Boggio, K. J., Petsko, G. A., Ringe, D. & Agar, J. N. Strategies for stabilizing superoxide dismutase (SOD1), the protein destabilized in the most common form of familial amyotrophic lateral sclerosis. *Proc. Natl. Acad. Sci. USA* **107**, 21394–21399 (2010).
11. Redler, R. *et al.* Glutathionylation at Cys-111 Induces Dissocation of Wild Type and FALS Mutant SOD1 Dimers. *Biochem* **50**, 7057–7066 (2011).
12. Sobott, F., Hernandez, H., McCammon, M. G., Tito, M. A. & Robinson, C. V. A tandem mass spectrometer for improved transmission and analysis of large macromolecular assemblies. *Anal. Chem.* **74** (2002).
13. Rostom, A. A., Tame, J. R. H., Ladbury, J. E. & Robinson, C. V. Specificity and interactions of the protein OppA: Partioning solvent binding effects using mass spectrometry. *J. Mol. Biol.* **296**, 269–279 (2000).
14. Furukawa, Y., Torres, A. S. & O'Halloran, T. V. Oxygen-induced maturation of SOD1: A key role for disulfide formation by the copper chaperone (CCS). *EMBO J.* **23**, 2872–2881 (2004).
15. Leinweber, B. *et al.* Aggregation of ALS mutant superoxide dismutase expressed in *Escherichia coli*. *Free Radic. Biol. Med* **36**, 911–918 (2004).
16. Lindberg, M. J., Normark, J., Holmgren, A. & Oliveberg, M. Folding of human superoxide dismutase: disulfide reduction prevents dimerization and produces marginally stable monomers. *Proc. Natl. Acad. Sci. USA* **101**, 15893–15898 (2004).
17. Tainer, J. A., Getzoff, E. D., Beem, K. M., Richardson, J. S. & Richardson, D. C. Determination and analysis of the 2 Å structure of copper, zinc superoxide dismutase. *J. Mol. Bio* **160**, 181–217 (1982).
18. Wang, Q., Johnson, J. L. & Agar, N. Y. R. N. A. J. Protein Aggregation and Protein Instability Govern Familial Amyotrophic Lateral Sclerosis Patient Survival. *PLoS Bio* **6**, 1508–1526 (2008).
19. Rumfeldt, J. A. O., Stathopulos, P. B., Chakrabartty, A., Lepock, J. R. & Meiering, E. M. Mechanism and thermodynamics of guanidinium cholride-induced denaturation of ALS-associated mutant Cu,Zn superoxide dismutases. *J. Mol. Bio* **355**, 106–123 (2006).
20. Perry, J. J. P., Shin, D. S., Getzoff, E. D. & Tainer, J. A. The structural biochemistry of the superoxide dismutases. *Biochim. Biophys. Acta* **1804**, 245–262 (2010).
21. Weisberg, S. J. *et al.* Compartmentalization of superoxide dismutase 1 (SOD1G93A) aggregates determines their toxicity. *Proc. Natl. Acad. Sci.* **109**, 15811–15816 (2012).
22. Barber, S. C. & Shaw, P. J. Oxidative stress in ALS: Key role in motor neuron injury and therapeutic target. *Free. Radic. Biol. Med.* **48**, 629–641 (2010).
23. Dalle-Donne, I., Rossi, R., Giustarini, D., Colombo, R. & Milzani, A. S-glutathionylation in protein redox regulation. *Free. Radic. Biol. Med* **43**, 883–898 (2007).

24. Tohgi, H. *et al*. Increase in oxidized NO products and reduction in oxidized glutathione in cerebrospinal fluid from patients with sporadic form of amyotrophic lateral sclerosis. *Neurosci. Lett.* **260**, 204–206 (1999).
25. Stansell, M. J. & Deutsch, H. F. The levels of catalase and of erythrocuprein in human erythrocytes. *Clin. Chim. Acta* **14**, 598–607 (1966).
26. Ruotolo, B. T., Benesch, J. L. P., Sandercock, A. M., Hyung, S. & Robinson, C. V. Ion mobility-mass spectrometry analysis of large protein complexes. *Nat. Protoc* **3**, 1139–1152 (2008).
27. Rose, R. J. *et al*. Quantitative analysis of the interaction strength and dynamics of human IgG4 half molecules by native mass spectrometry. *Structure* **19**, 1274–1282 (2011).

Acknowledgments

We thank the Oliveberg Group, (Stockholm University, Sweden) for kindly providing the SOD1 expression vectors. JJY is supported by the Australian Research Council in the form of a DECRA Fellowship, and by NHMRC project grant 1003032. LM is supported by a University of Wollongong Matching Scholarship. Research facilities were provided by the University of Wollongong Illawarra Health and Medical Research Institute.

Author contributions

JAA and JJY conceptualized, designed and supervised the study. LM performed experiments, analyzed data, and wrote the initial manuscript draft. JAA revised and finalized the manuscript for submission.

Additional information

Supplementary information accompanies this paper at http://www.nature.com/scientificreports

Competing financial interests: The authors declare no competing financial interests.

How to cite this article: McAlary, L., Yerbury, J.J. & Aquilina, J.A. Glutathionylation potentiates benign superoxide dismutase 1 variants to the toxic forms associated with amyotrophic lateral sclerosis. *Sci. Rep.* **3**, 3275; DOI:10.1038/srep03275 (2013).